The 19th Conference of Mechanical Engineering Network of Thailand
19-21 October 2005, Phuket, Thailand

Effect of Thermosyphon Evaporative Length on Temperature Reduction of Cool Water

Nammont Chotivisarut* and Tanongkiat Kiatsiriroat

Department of Mechanical Engineering, Faculty of Engineering, Chiang Mai University,
Chiang Mai, Thailand 50200
*E-mail: nammont4426409@hotmail.com

Abstract
The objective of this study is to evaluate thermal characteristics of vertical thermosyphon heat pipe, generating cool water at its evaporative section. The effect of the evaporative length on the heat transfer of thermosyphon heat pipe has studied experimentally and numerically by CFD. In the experimental study, three copper thermosyphon heat pipes with R-134a inside of 19.05 mm. diameter with 1.00, 0.85, 0.70 m. length are used to extract heat from 3.5 L. water, containing in a well-insulated vessel. At the condenser part, there is cooling water, maintained at 10 °C. The heat transfer coefficients of water, having higher evaporative length increase monotonously with the ratio of evaporative length to the water level. The value of the heat transfer coefficients are used to estimate the history of water temperature in the vessel. The CFD simulated temperature agrees very well with the experimental data within 8.0 percent errors.
Keywords: thermosyphon, temperature reduction, cool water, heat pipe

1. Introduction

Nowadays, changing of building style and function has led to a greater dependence on artificial forms of lighting, heating, cooling and ventilation within modern buildings. Recent environmental concerns have however, led to a greater focus on traditional passive methods of solar control, natural ventilation and other passive cooling methods. Designers, architects and engineers have adapted many traditional basic principles to fit in with the modern office environment, both in terms of building practices and materials and in the way in which we work today, often resulting in innovative design solutions.

One of the passive cooling methods is night sky cooling technique, which has been studied by many researchers. Vimolrat [1] has designed the new alternative night sky cooling systems by using the thermosyphon attached with the radiator, with no water circulation as shown in Figure 1.

This work is to extend the study of Vimolrat by considering the effect of evaporative length on the heat extraction rate of the cool water storage. The CFD simulation is also carried out to evaluate the water temperature.

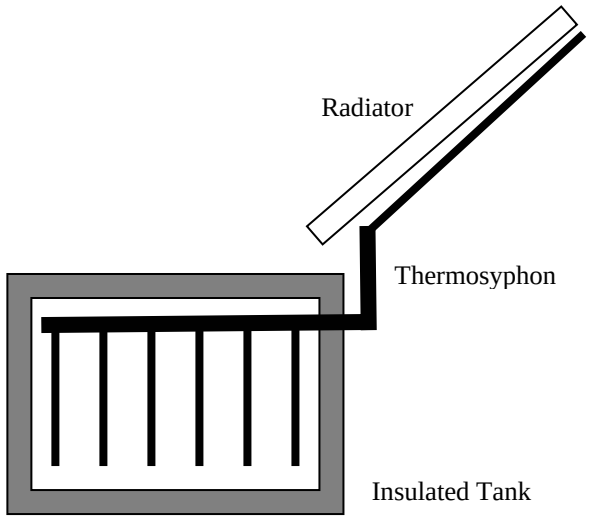

Figure1. Schematic drawing of night sky cooling system by using a thermosyphon radiator.

2. Two-Phase Closed Thermosyphon Heat Pipe

The closed two-phase thermosyphons is an effective heat transfer device that obtains its heat from the evaporator section by means of the evaporating mechanism and, then releasing the heat out at the condenser section by means of the condensing phenomenon. Since the latent heat of vaporization of the working fluid is relatively high, a large amount of heat can be transported through the thermosyphon. The thermosyphon can mainly operate under the assistance of the gravity; as shown in Figure 2. The unit can be separated into 3 parts as evaporator, adiabatic and condenser sections.

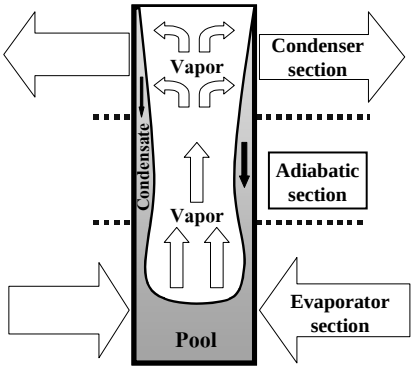

Figure2. Thermosyphon [2].

The actual overall rate of heat transfer, Q is then related by:

$$Q = \frac{\Delta T}{Z_{total}}, \qquad (1)$$

where Q is the rejected heat (W),

ΔT is the effective temperature difference between the heat source and the heat sink (°C):

$$\Delta T = T_{so} - T_{si} - \Delta T_h , \qquad (2)$$

where Tso is the heat source temperature (◦C),

Tsi is the heat sink temperature (◦C),

ΔT_h is the mean temperature difference due to hydrostatic head (°C).

where Z_{total} is the overall thermal resistance of the thermosyphons can be represented by the idealized network of thermal resistances Z_1 to Z_{10} as shown in Figure 3.

where Z_1 and Z_9 are the thermal resistance between the heat source and the evaporator and the condenser external surface and the heat sink respectively

Z_2 and Z_8 are the thermal resistances across the thickness of the contains wall in the evaporative and the condenser respectively

Z_3 and Z_7 are the internal resistances due to pool and film boiling of the working fluid

Z_{3p} is the resistance from pool boiling

Z_{3f} is the resistance from film boiling at the evaporator section

Z_4 and Z_6 are the thermal resistance those occur at the vapor liquid interface in the evaporator and the condenser respectively

Z_5 is the effective thermal resistance due to the pressure drop of the vapor as it flows from the evaporative to the condenser

Z_{10} is the axial thermal resistance of the wall of the container.

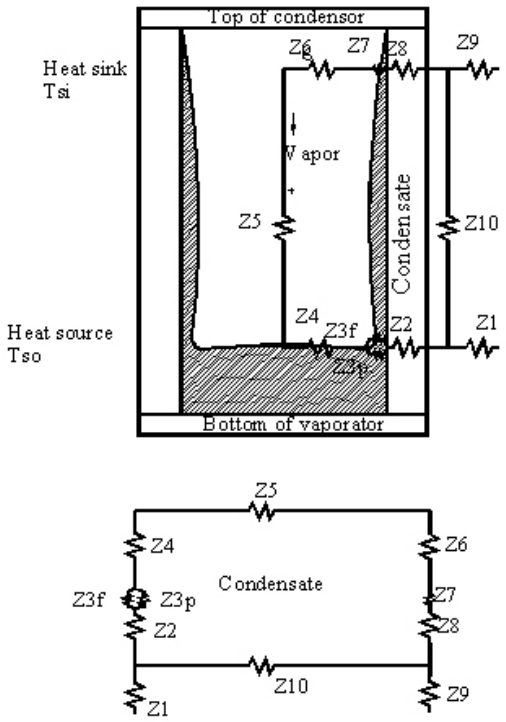

Figure3. Thermal resistance and their locations.

The details and calculated methods of all Z are shown in all available designed text books [3].

3. Experimental Setup

The experimental sets were based on three vessel of 3.5 L. of water, containing in a well-insulated vessel. In this experimental study, three copper thermosyphon heat pipes having R-134a inside with 19.05 mm. diameter and 1.00, 0.85, 0.70 m. length were used to extract heat from water in a water storage. The condenser length (L_c) and the adiabatic length (L_a) of each thermosyphon heat pipe were at 0.45 and 0.10 m. respectively, when the evaporative length (L_e) is varied. The L_e/L_c ratios of three thermosyphon heat pipe were 1.00, 0.67 and 0.33 respectively. The initial water temperature in each vessel was at 45 °C. At the condenser part, there was cooling water, maintained at 10 °C by a cold bath, as shown in Figure 4.

Fluid and surface temperature were measured by IC sensors, calibrated individually so that the differential error of measurement was less than 0.5 °C. All data were transferred to a 16 channel data-logger and collected every 10 minutes. The fluid and the surface temperatures were multi-pointed measurement and used the average value for calculation.

The water temperature data from an experiment were used to calculate the rejected heat by the thermosyphon heat pipe by:

$$Q = \frac{mC_p(T_{w,t} - T_{s,t+\Delta t})}{\Delta t}, \qquad (3)$$

where Q is the rejected heat (W),
m is the mass of water in study time step (kg),
Cp is the heat capacity of water (4179 kJ/kg K),
Tw is the water temperature (°C),
Δt is the time interval (s).

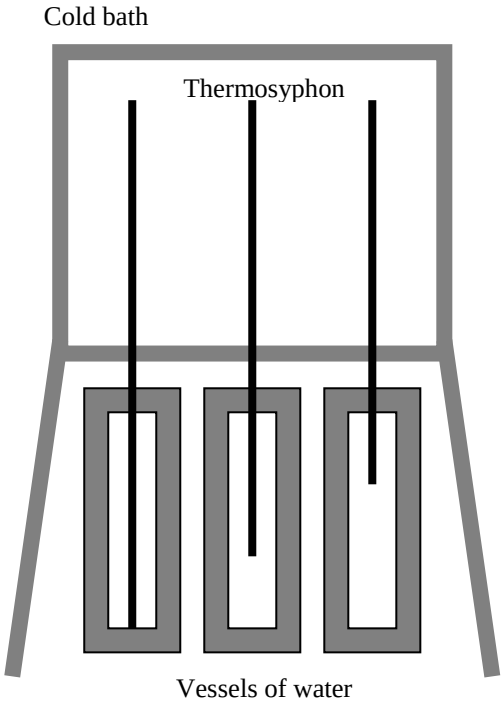

Figure4. Schematic drawing of the experimental setup.

The rejected heat was used to calculate the heat transfer coefficients around each thermosyphon heat pipe as:

$$h = \frac{Q}{A(T_w - T_s)}, \qquad (4)$$

where h is the heat transfer coefficients (W/ m^2 K),
A is thermosyphon heat pipe surface area (m^2),
T_s is the thermosyphon surface temperature (°C).

4. Computation Fluid Dynamics (CFD)

A cell-centered control volume solution approach was deployed. This approach implies that the discrete equations are formulated by evaluating and integrating the fluxes across the faces that surround each control volume. In addition, this calculated system uses a pressure-based methodology in which the pressure becomes one of the dependent equations evaluated at each cell. This method allows the solutions for incompressible problems where pressure is loosely coupled to density.

The computation domains were the water in each 0.10 m. width x 0.45 m. height vessels, which were divide into 16 x 45 grids. The adiabatic boundary conditions are set around the computation domains, when the convective boundary conditions are set at the thermosyphon surfaces, using the average heat transfer coefficients from each experiment as the input data in the CFD simulation. The calculated outputs were vector flow fields and also fluid temperature at each time steps.

5. Result and Discussion

The experimental results of water temperature and rejected heat between thermosyphon heat pipe, having L_e/L_c = 1.00, 0.67 and 0.33 are shown in Figures 5 and 6, respectively. Due to the larger evaporative part surface area, the L_e/L_c = 1.00 thermosyphon heat pipe unit can reject heat from the system more than the L_e/L_c = 0.67 and L_e/L_c = 0.33 uint by 14% and 45%, respectively. This condition also gives the lowest water temperature.

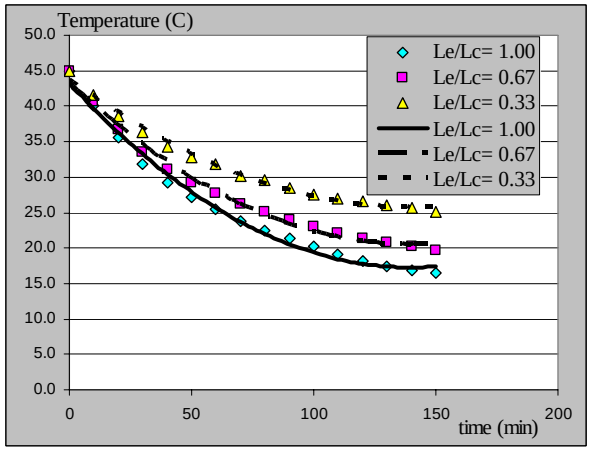

Figure5. The experimental result of water temperature between L_e/L_c = 1.00, 0.67 and 0.33.

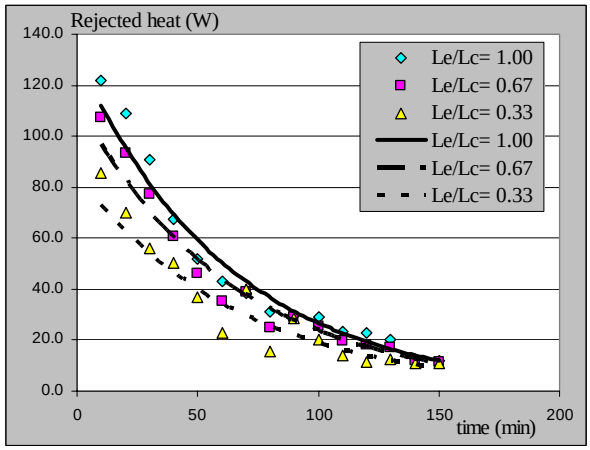

Figure6. The experimental result of rejected heat between L_e/L_c = 1.00, 0.67 and 0.33.

Figures 7, 8 and 9 show the water temperatures from the CFD that agree very well with the experimental results within 8% errors, with the 3.1% average error. But when comparing the experimental and the theoretical study, the average error was 12.8%. Both maximum error occurred when L_e/L_c = 0.33.

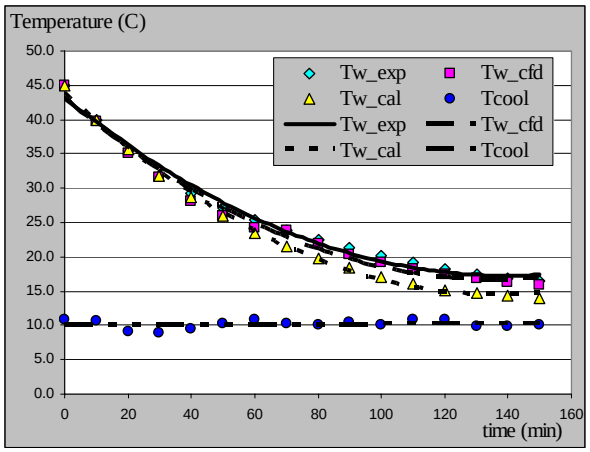

Figure7. Water temperature of the experiment, CFD and theoretical study when $L_e/L_c = 1.00$.

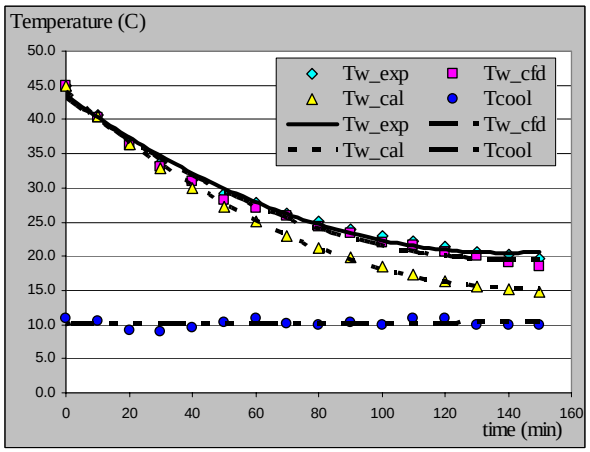

Figure8. Water temperature of the experiment, CFD and theoretical study when $L_e/L_c = 0.67$.

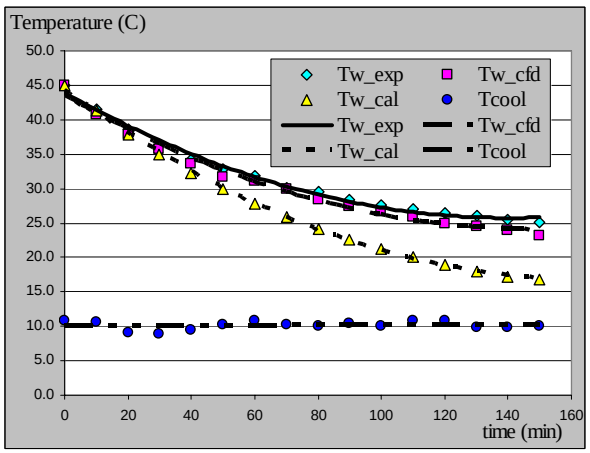

Figure9. Water temperature of the experiment, CFD and theoretical study when $L_e/L_c = 0.33$.

The rejected heat in the experiment and CFD simulation can be found after knowing the water temperature data at each time steps by using equation (3). As shown in Figures 10, 11 and 12, the experimental and CFD simulated result have 10.5% average error. But when comparing the experimental and theoretical study, the average error was 30.9%. Both maximum error occurred when $L_e/L_c = 0.33$.

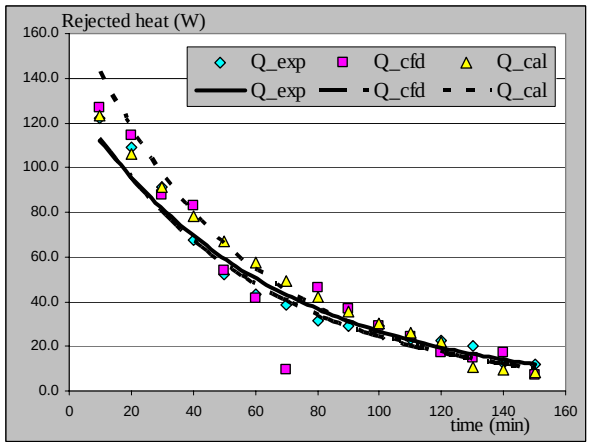

Figure10. Rejected heat of the experiment, CFD simulation and theoretical study when $L_e/L_c = 1.00$.

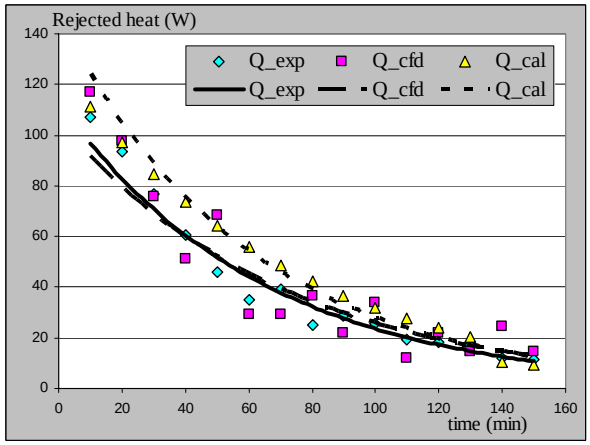

Figure11. Rejected heat of the experiment, CFD simulation and theoretical study when $L_e/L_c = 0.67$.

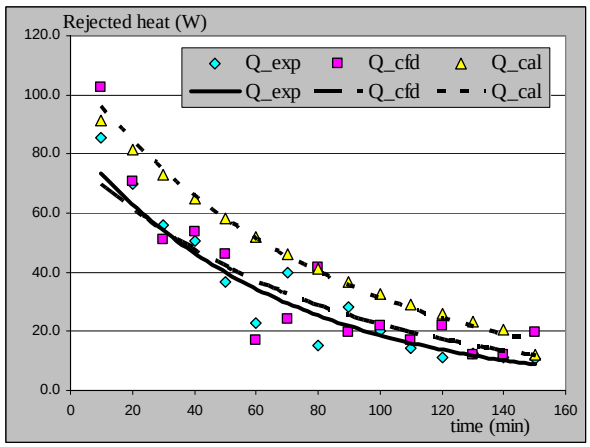

Figure12. Rejected heat of the experiment, CFD simulation and theoretical study when $L_e/L_c = 0.33$.

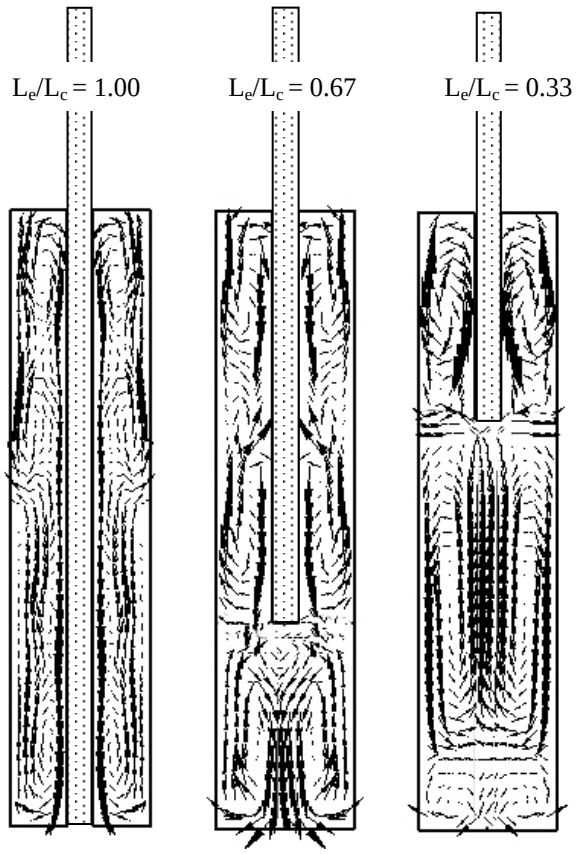

Figure13. The vector flow fields at time = 30 minutes.

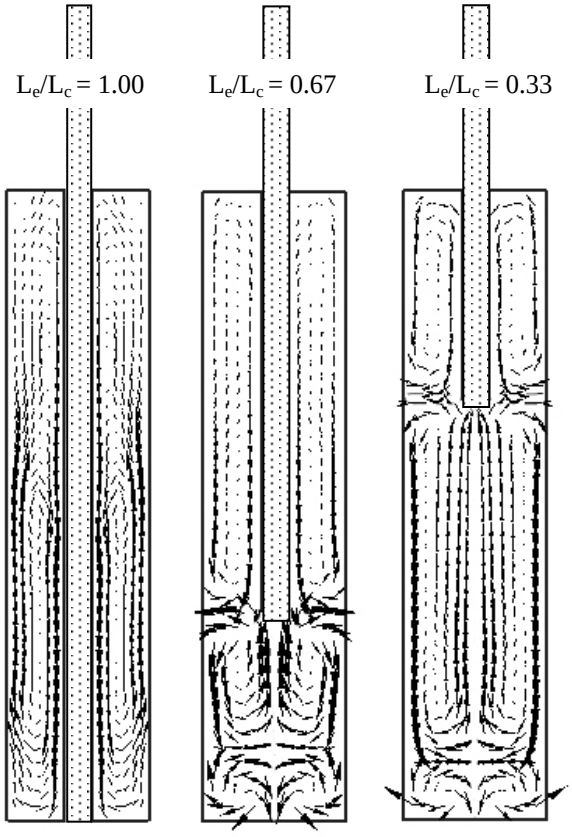

Figure14. The vector flow fields at time = 150 minutes.

The resulted error in each cased study can be explained by the CFD simulation. Figures 13 and 14 show the vector flow fields of all case studies at time 30 and 150 minutes, respectively. When L_e/L_c = 1.00, the vector flow fields around the thermosyphon heat pipe was one loop circulation, that the water in the vessel could flow throughout the vessel. This factor leads to high accuracy when using measured water temperature at each water level to calculate the average heat transfer coefficients to be the input data in the CFD simulation and theoretical study. When L_e/L_c = 0.67 and 0.33, the vector flow fields around the thermosyphon heat pipe were clearly divided into three regions. This unsatisfied circulation leading to an error when using measured water temperature in the studies, cause of the temperature different in each loop. As mention above, using the average heat transfer coefficients from an experiment as the input in both CFD simulation and theoretical study give the highest accuracy in the case L_e/L_c = 1.00, when be lower L_e/L_c will be lower in an accuracy.

6. Conclusion

This study has shown the effect of the evaporative length on the heat transfer of thermosyphon heat pipe. Due to the larger evaporative part surface area, the L_e/L_c = 1.00 thermosyphon heat pipe unit can reject heat from the system more than the L_e/L_c = 0.67 and L_e/L_c = 0.33 uint by 14% and 45%, respectively. This condition also gives the lowest water temperature.

Moreover, this study has also shown the significant of using average heat transfer coefficients from the experiment as the input in the CFD simulation and theoretical study to find water temperature and rejected heat in the un-uniformed heat source temperature situation. When comparing with the experiment, the resulted error from the theoretical study seems to be much higher than that from the CFD simulation. The maximum error always occurs in the case study when L_e/L_c = 0.33. The vector flow fields and water temperature from CFD simulation were used to explain the phenomenon.

Acknowledgements

This research is financially supported by the Thailand Research Fund, contract no. PHD/ 0273/ 2545

References

[1] Vimolrat C., Nocturnal Water Cooling for Trout Fish Pond During Hatching Period, Graduate School, Chiang Mai University, 2004.

[2] Dunn, P. D. and Reay, D. A., Heat Pipe 3rd Edition, Pergamon Press Ltd., U.K., 1982.

[3] Engineering Sciences Data Unit Item Number 81038: Heat pipes-performance of two-phase closed thermosyphons, Specialised Printing Services Limited, London, 1981.